Eur. Phys. J. B **34**, 41–46 (2003)
DOI: 10.1140/epjb/e2003-00194-3

THE EUROPEAN PHYSICAL JOURNAL B

Magnetic anisotropy of ferromagnetic layered manganites

J.-P. Renard[1,a] and M. Velázquez[1,2,b]

[1] Institut d'Électronique Fondamentale[c], bâtiment 220, Université Paris-Sud, 91405 Orsay Cedex, France
[2] Laboratoire de Physico-Chimie de l'État Solide[d], bâtiment 414, Université Paris-Sud, 91405 Orsay Cedex, France

Received 12 December 2002 / Received in final form 29 April 2003
Published online 23 July 2003 –

Abstract. The magnetic anisotropy of the ferromagnetic layered manganites $La_{2-2x}Sr_{1+2x}Mn_2O_7$ is investigated. For $x = 0.4$, the easy-plane anisotropy comes out predominantly from dipolar interaction but it is partly cancelled out by a significant uniaxial magnetocrystalline anisotropy. This latter one is discussed on the basis of a simple single ion model and compared to existing experimental data in ferromagnetic manganites.

PACS. 75.10.Dg Crystal-field theory and spin Hamiltonians – 75.30.Gw Magnetic anisotropy – 75.30.Vn Colossal magnetoresistance

1 Introduction

The layered manganites of general formula $La_{2-2x}Sr_{1+2x}Mn_2O_7$ with $0.3 \leq x \leq 0.44$ exhibit a phase transition to a metallic ferromagnetic phase at low temperature with a strongly anisotropic electrical conductivity [1]. This transport anisotropy comes out from the structure consisting in magnetic Mn bilayers parallel to the *ab* plane separated from each other by a non magnetic (La,Sr)O layer. This also confers a two-dimensional (2d) character to the magnetism leading to relatively low T_c values and to spin correlations extending well above T_c [2,3]. It is well known that the transition of 2d-magnets with short range interactions is quite sensitive to magnetic anisotropy. Indeed, the 2d-Ising model undergoes a transition to a phase with long range order (LRO) at finite temperature, the 2d-Heisenberg model has a correlation length diverging at $T = 0$ and no LRO for $T > 0$, while the 2d-XY model exhibits the Kosterlitz- Thouless transition at finite temperature to a phase with infinite correlation length but without LRO.

Even if in the layered manganites the ferromagnetic transition is likely induced by the small exchange interaction between the adjacent Mn bilayers [3], the magnetic anisotropy is quite important for governing the magnetic properties and thus deserves to be studied. The two main sources of anisotropy are the combined effect of crystal field and spin-orbit coupling and the dipolar interaction between the magnetic moments of the Mn ions. In this paper, the contributions of these mechanisms, respectively the magnetocrystalline anisotropy and the dipolar anisotropy are evaluated and compared to the experimental data, in particular for $La_{1.2}Sr_{1.8}Mn_2O_7$.

2 Magnetocrystalline anisotropy

In doped manganites, the Mn ions are in a state of mixed valency, Mn^{3+}-Mn^{4+}. The hopping process of e_g electrons *via* the O^{2-} $2p$ orbitals between neighboring Mn^{3+} and Mn^{4+} is responsible for electrical conductivity and ferromagnetic double exchange [4,5]. For sake of simplicity, we shall consider the manganite is composed of Mn^{3+} and Mn^{4+} ions in respective proportion $1 - x$ and x and the magnetic anisotropy is the weighted sum of the single ion anisotropy of Mn^{3+} and Mn^{4+}. The Mn ion is surrounded by an octahedron of oxygen atoms, more or less axially distorted depending on x. The distortion is strong in Mn^{+3} rich manganites such as $LaMnO_3$ [6,7] due to the large Jahn-Teller effect of Mn^{+3} and it gradually decreases with increasing the concentration x in Mn^{4+}. The crystal field experienced by the Mn ion is thus composed of two contributions: a large cubic contribution since the symmetry is predominantly cubic, and a smaller tetragonal contribution roughly proportional to the axial elongation of the oxygen octahedron. This latter one joined to the spin-orbit coupling is at the origin of magnetic anisotropy.

Let us first consider the case of a Mn^{3+} ion which, following Hund's rules, has a total spin $S = 2$ and a total orbital moment $L = 2$. The five-fold orbital degeneracy

[a] e-mail: jean-pierre.renard@ief.u-psud.fr
[b] *Present address*: Centre Interdisciplinaire de Recherche Ions-Lasers, UMR 6637 CNRS/CEA/ISMRA, groupe "Matériaux et Instrumentation Laser", 6 Boulevard du Maréchal Juin, 14050 Caen Cedex 4, France
[c] UMR 8622 CNRS
[d] UMR 8648 CNRS

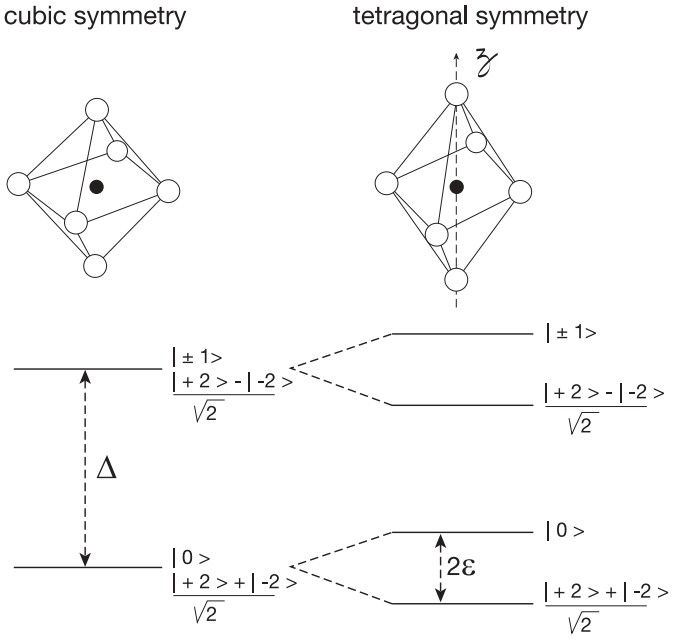

Fig. 1. Energy level diagram and orbital eigenstates of Mn^{3+} in a crystal field of cubic and tetragonal symmetry.

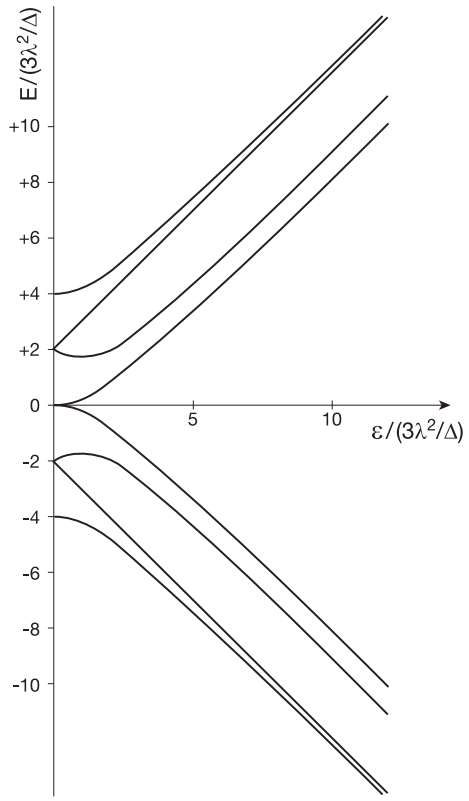

Fig. 2. Dependence of the spin-orbit split energy levels of the ground state of Mn^{3+} on the tetragonal splitting 2ε.

$(L_z = -2, -1, 0, 1, 2)$ is partly lifted by the crystal field [8] as shown in Figure 1. In particular for elongated MnO_6, the tetragonal contribution gives rise to an orbital singlet ground state $|G\rangle = (|2\rangle + |-2\rangle)/\sqrt{2}$ and to a first orbital excited state $|0\rangle$, 2ε higher in energy, which join together for purely cubic symmetry. As an effect of spin-orbit coupling $\lambda \mathbf{L}\cdot\mathbf{S}$, the five-fold spin degeneracy of $|G\rangle$ is partly lifted. The energy shifts are given to the second order perturbation by:

$$\Delta E^{(2)} = \Sigma(|\langle G, S_z = M_S|\lambda \mathbf{L}\cdot\mathbf{S}|n\rangle|^2)/(E_0 - E_n) \quad (1)$$
$$S_z = M_S$$

in which the summation is performed on all the excited states $|n\rangle$ of energy E_n and z is the tetragonal axis *i.e.* the elongation axis of the oxygen octahedron. The corresponding energy shifts of the ground state sublevels are:

$$\Delta E = -6\lambda^2/\Delta; \quad \Delta E = -9\lambda^2/\Delta; \quad \Delta E = -18\lambda^2/\Delta \quad (2)$$
$$S_z = 0 \qquad S_z = \pm 1 \qquad S_z = \pm 2$$

where Δ is the splitting by the cubic crystal field. Save on an additive constant, $-6\lambda^2/\Delta$, the energies of these sublevels are reproduced by the usual single ion anisotropy spin Hamiltonian $H_{MA} = D(S_z)^2$ with $D = -3\lambda^2/\Delta$. Surprisingly, the size D of the magnetic anisotropy does not depend on the magnitude of the tetragonal term of the crystal field which nevertheless is necessary for its existence. This apparent paradox can be understood looking at the splitting of the first orbital excited state, $|0\rangle$, by the spin-orbit coupling. The second order perturbation calculation leads to $D(S_z)^2$ with $D = +3\lambda^2/\Delta$ which exactly cancels out that of the ground state. Thus, the resulting single ion anisotropy vanishes for cubic anisotropy at which the two levels join together. The detailed dependence of the spin orbit multiplets of lowest energy on the tetragonal splitting 2ε is shown in Figure 2. For perfect cubic symmetry, $\varepsilon = 0$, the ground level is split into five $6\lambda^2/\Delta$ apart equidistant levels by the spin orbit coupling [9] which evolve into the two multiplets $D(S_z)^2$ mentioned before for $\varepsilon \gg 3\lambda^2/\Delta$. The corresponding second order perturbation calculation is given in appendix. Since $3\lambda^2/\Delta \approx 2$ K in manganites [10], a tiny distortion of the oxygen octahedron is enough to achieve $\varepsilon \gg 3\lambda^2/\Delta$. Calling P_0 and P_1 the respective probabilities of occupation of the states $(|2\rangle + |-2\rangle)/\sqrt{2}$ and $|0\rangle$, the anisotropy can be written as $D_{eff}(S_z)^2$ with $D_{eff} = -3\lambda^2(P_0 - P_1)/\Delta$ in agreement with the previous work of Matsumoto [11]. $P_0 - P_1$ is simply given at 0 K by $P_0 - P_1 = 2\varepsilon/W$ where W is the width of the Mn^{3+} levels for a rectangular profile and $2\varepsilon < W$. Finally the effective single ion anisotropy for $2\varepsilon \ll W$ can be approximated by:

$$D_{eff} = -3(2\varepsilon/W)\lambda^2/\Delta. \quad (3)$$

The Mn^{4+} single ion anisotropy in a similar crystal field is less subtle. Indeed, the orbital ground state in cubic symmetry is a singlet and the splitting, ε', of the first excited state by the tetragonal crystal field appears explicitly in the expression of D [12]:

$$D = -8\lambda^2\varepsilon'/\Delta'^2 \quad (4)$$

in which Δ' is the energy of the first excited level and for $\varepsilon' \ll \Delta'$.

Since Mn^{4+} is not a Jahn-Teller ion, it undergoes a tetragonal distortion much smaller than in the case of Mn^{3+} and then, its contribution to the magnetocrystalline anisotropy is likely negligible.

3 Dipolar anisotropy

The magnetic moments of the Mn ions in manganites being relatively large, 3–4 μ_B where μ_B is the Bohr magneton, their dipolar interaction can contribute to magnetic anisotropy. However, in 3*d* manganites the Mn lattice is close to a cubic lattice for which the dipolar anisotropy vanishes in the case of ferromagnetic order. On the other hand, the dipolar anisotropy is important in manganites with layered structure such as $La_{2-2x}Sr_{1+2x}Mn_2O_7$. The energy of interacting point dipoles all parallel located at the Mn sites was computed for different orientations of the magnetization. The summation was performed within a sphere of radius R, and R was increased until the convergence of the sum was achieved. It is found that the dipolar interaction leads to *ab* as easy plane for the magnetization and *c* as hard axis. For $x = 0.4$, with $a = b \approx 0.387$ nm, $c \approx 2.012$ nm and $\mu = (3.55 \pm 0.05)\ \mu_B$/Mn [3], the calculated dipolar anisotropy energy per unit volume is $K_D \sin^2\theta$ with $K_D = -4.35 \times 10^5$ erg/cm^3 and $|2K_D|/M_S \approx 1.98$ kOe at 0 K, where M_S is the saturation magnetization and θ stands for the angle between the magnetization and the *c*-axis. For $0.32 \leq x \leq 0.44$, K_D does not appreciably change since the unit cell is nearly independent on x and the magnetic moment only slightly increases on decreasing x.

4 Results and discussion

The manganites with strong distortion of the oxygen octahedron have a large magnetic anisotropy. Indeed, the anisotropy field, H_A, of antiferromagnetic $LaMnO_3$ deduced from the measured spin-flop field of a single crystal is $H_A \approx 37$ kOe. It is consistent with the magnetocrystalline anisotropy of Mn^{3+}, $D = -3\lambda^2/\Delta$ which leads to $|D/k_B| \approx 1.95$ K for $\lambda/k_B = 127$ K and $\Delta k_B \approx 25\,000$ K [10] where k_B is the Boltzmann constant. As a matter of fact, the magnetism of $LaMnO_3$ is complex due to two non equivalent Mn^{3+} sites with different directions of axial MnO_6 elongation and to a significant Dzyaloshinsky-Moriya interaction [10,13]. This is not the case of $La_{1.2}Sr_{1.8}Mn_2O_7$ in which all the MnO_6 octahedra are elongated along the same axis *c*. On reducing the distortion of $LaMnO_3$ by substitution of alkaline earth ion to La, the magnetic anisotropy strongly decreases. For instance in a ferromagnetic single crystal of $La_{0.67}Sr_{0.33}MnO_3$, a uniaxial anisotropy energy $K_u \sin^2\theta$ with $K_u \approx 9 \times 10^4$ erg/cm^3 at $T = 100$ K was observed, corresponding to an anisotropy field of about 300 Oe [14]. It was interpreted as being due to the rhombohedral crystal distortion.

However, in epitaxial thin films of same composition, the magnetic anisotropy can be enhanced by one order of magnitude or more, depending on substrate type and orientation [15–20]. This enhancement which likely arises from the distortion of the oxygen octahedron induced by the epitaxial strains corroborates the magnetocrystalline origin of the anisotropy. The films of $La_{1-x}Sr_xMnO_3$ (LSMO) and of $La_{1-x}Ca_xMnO_3$ (LCMO) with $x = 0.30-0.33$ experience in the film plane extensive strain when deposited on $SrTiO_3$ (STO) and compressive strain when deposited on $LaAlO_3$ (LAO). The resulting distortion of the MnO_6 octahedra induces uniaxial magnetocrystalline anisotropy which favors the film plane as magnetization easy plane for films on STO (compressed octahedron) and perpendicular magnetization for films on LAO (elongated octahedron).

In the ferromagnetic layered manganites $La_{2-2x}Sr_{1+2x}Mn_2O_7$, the MnO_6 octahedra are slightly elongated along the *c* axis, perpendicular to the Mn layers. The elongation quantified by the ratio ρ of the averaged apical and the equatorial Mn-O bond lengths decreases with increasing x [21–23]. So far, quantitative magnetic anisotropy data have been reported only for $x = 0.32$ [24]. At low temperature, the uniaxial magnetocrystalline anisotropy, $K_M = 7 \times 10^5$ erg/cm^3, dominates the dipolar anisotropy leading to c as easy axis. In this work, the experimental data were fitted to the anisotropy energy $K_1 \sin^2\theta + K_2 \sin^4\theta$ with $K_2 \approx K_1$. A ratio K_2/K_1 close to 1 is not expected since K_2 is a higher order term than K_1 in the expansion of the anisotropy energy in successive powers of the components of the unit vector of the magnetization. This may be explained by the reduced value of K_1 due to a cancellation of the magnetocrystalline anisotropy by the dipolar one and by a possible distribution of K_1 by local disorder. Indeed, it has been shown that spatial fluctuations of the first order anisotropy constant in ferromagnetic films such as Co/Au(111) give rise to a higher anisotropy term [25]. We consider here the case of the easy-plane ferromagnet $La_{1.2}Sr_{1.8}Mn_2O_7$ ($x = 0.4$). The magnetic anisotropy deduced from the magnetization curve in field applied along *c* is $K = -2.87 \times 10^5$ erg/cm^3 [3]. The magnetic anisotropy comes out predominantly from the dipolar interaction. From the dipolar anisotropy calculated in Section 3, $K_D = -4.35 \times 10^5$ erg/cm^3, one obtains the following magnetocrystalline anisotropy: $K_M = K - K_D = 1.48 \times 10^5$ erg/cm^3.

The data of distortion and magnetocrystalline anisotropy in $La_{2-2x}Sr_{1+2x}Mn_2O_7$ and in various epitaxial thin films of LSMO and LCMO are reported in Table 1. The distortion δ is defined by $\delta = \rho - 1$ for $La_{2-2x}Sr_{1+2x}Mn_2O_7$ and by $\delta = c/a - 1$ for epitaxial thin films, *c* and *a* being the lattice parameter respectively perpendicular and parallel to the film plane. We suppose that the distortion of the MnO_6 octahedron is identical to the one of the unit cell in epitaxial thin films. This is just a simple hypothesis required by the lack of detailed crystallographic experimental data on strained films. For an elongation of MnO_6, $\delta > 0$, whereas $\delta < 0$ for

Table 1. Distortion δ (at 20 K for the single crystals and at room temperature for the thin films), uniaxial magnetocrystalline anisotropy constant K_M and ratio $2K_M/M_S$ (where M_S is the saturation magnetization) and temperature T at which K_M and M_S were determined in two $La_{2-2x}Sr_{1+2x}Mn_2O_7$ single crystals with $x = 0.4$ and 0.32 and in a series of epitaxial manganite thin films. The thickness of the manganite thin films is given in brackets. The substrate orientation is (001). T_C of the sample is also given when available.

System	δ (%)	K_M (10^5 erg/cm^3)	$2K_M/M_S$ (kOe)	T/T_C (K)	Ref.
$La_{1.2}Sr_{1.8}Mn_2O_7$	+1.6	+1.5	+0.67	20/108	[3,22]
$La_{1.36}Sr_{1.64}Mn_2O_7$	+3.2	+7	+3.2	20/112	[23,24]
LSMO/LAO (7 nm)	+2.3	+3	+2.7	100/270	[20]
LSMO/LAO (20 nm)	+0.96	+4	+2.2	100/310	[20]
LSMO/LAO (25 nm)	+5.3	>2.5	>2.5	5/300	[18]
LCMO/LAO (25 nm)	+1.9	+12	+7.5	5/?	[17]
LCMO/LAO (58 nm)	+5.5	+14(±8)	+4.7(±2.7)	150/350	[19]
LSMO/STO (25 nm)	−1.4	−10	−4	5/320	[18]
LCMO/STO (25 nm)	−1.4	−18	−8	5/?	[17]
LCMO/STO (58 nm)	−1.8	−15	−6	5/170	[16]

a compression. In addition to the anisotropy constant K_M, the ratio $2K_M/M_S$ where M_S is the saturation magnetization was also given in Table 1. This ratio which represents an anisotropy field for $K_M > 0$ is likely less dependent on the differences between the studied manganites since it is only weakly dependent on the number of Mn atoms per volume unit. Table 1 clearly demonstrates the correlation between magnetic anisotropy and distortion but the data are still scarce for establishing the quantitative dependence. For $La_{2-2x}Sr_{1+2x}Mn_2O_7$, the magnetocrystalline anisotropy is about four times larger for $x = 0.32$ than for $x = 0.4$ whereas δ is only twice. This seems to rule out a simple proportionality law. However, discrepancies between the measurements performed by different research teams on crystals of the same composition, for T_c for instance, mainly due to the difficulty of growing high quality single crystals, force one to be careful to compare the data on single crystals having the same thermal history. To date, this remains almost impossible, for the current literature does not provide all the relevant informations on the samples. The situation is still worse for thin films due to important effects of microstructure and interfaces. In particular, their magnetization is often severely reduced with respect to bulk manganites by dead layers at the interfaces.

From equation (3), an order of magnitude of the uniaxial magnetocrystalline anisotropy of the ferromagnetic manganites can be estimated. The corresponding anisotropy field $H_A = 2K_M/M_S$ is expressed as $H_A = 2(1-x)|D_{eff}|[1-1/(2S)]S^2/g\mu_B S$. With $3\lambda^2/\Delta = 1.95$ K, $S = 2, x = 0.4$ and $g = 2$, one obtains H_A(kOe) $\approx 26 \times 2\varepsilon/W$. Typically, $W \sim 1$ eV and $2\varepsilon/W \sim 10^{-1}$ for a few % distortion, which gives a right order of magnitude for $H_A, \sim 2.6$ kOe. A more rigorous first-principles calculation of uniaxial anisotropy of manganite films on STO and LAO [26] is in agreement with the experimental data and support our simple model of localized spins.

It is surprising that the magnetic anisotropy of manganites can be reasonably interpreted by the ionic model of localized electrons. Indeed, it is generally admitted that this model is valid for undoped insulating manganites but that a band model of itinerant e_g electrons is more suited for doped metallic phases. However, the optical spectra of manganites do not exhibit drastic changes from insulating to metallic phases, except in the far infrared. The manganites are, as a matter of fact, bad metals. For the presently studied $La_{1.2}Sr_{1.8}Mn_2O_7$, the resistivity measured along the c axis does not fulfil the Ioffe-Regel criterion, which means that the electron mean free path along c is smaller than the Mn interatomic distance and thus the electrons are only weakly delocalized [27]. This is confirmed by the ^{55}Mn NMR spectra which exhibit lines typical of a non-metallic phase [28].

5 Summary

We have shown that the magnetocrystalline anisotropy of the manganites is reasonably accounted for by a simple single ion model. The single ion anisotropy DS_z^2 arises from the combined effect of the spin-orbit coupling and of the tetragonal distortion of the MnO_6 octahedron. For Mn^{3+}, D is negative for an elongation and positive for a compression. The respective easy axis and easy plane anisotropy is in agreement with the existing experimental data in layered manganites $La_{2-2x}Sr_{1+2x}Mn_2O_7$ and strained epitaxial thin films of (La,Ca)MnO_3 and (La,Sr)MnO_3. The easy plane magnetic anisotropy of $La_{1.2}Sr_{1.8}Mn_2O_7$ was found to be predominantly due to dipolar interaction but this latter one is partly cancelled out by a significant uniaxial magnetocrystalline anisotropy which has been precised. Finally, the dependence of the spin-orbit splitting of the ground energy level of Mn^{3+} on the tetragonal splitting has been calculated.

We wish to thank Dr P. Beauvillain for the calculation of dipolar anisotropy and Dr G. Fishman for illuminating explanations about the second order perturbation treatment of degenerate levels.

Appendix

In a crystal field of cubic symmetry, the ground energy level of Mn^{3+} has a ten-fold degeneracy, the corresponding ground subspace being defined by the eigenvectors $|(|2\rangle + |-2\rangle)/\sqrt{2}, S_z = M_S\rangle$ and $|0, S_z = M_S\rangle$ where M_S, the eigenvalue of the spin component S_z, is equal to 0, ± 1 and ± 2. All matrix elements of the spin-orbit coupling $\lambda \mathbf{L}\cdot\mathbf{S}$ being equal to zero within this subspace, it is necessary to build the matrix of $\lambda \mathbf{L}\cdot\mathbf{S}$ in the ground subspace to the second order of perturbation. In addition to the diagonal matrix elements given by equation (1), non diagonal elements have to be considered. Their general expression is the following:

$$\langle i|H'|j\rangle = \sum \langle i|H'|n\rangle\langle n|H'|j\rangle/(E_0 - E_n) \qquad (A.1)$$

in which H' is the perturbating Hamiltonian, $|i\rangle$ and $|j\rangle$ are eigenvectors of the ground subspace and the summation is performed on all the excited states $|n\rangle$ of energy E_n. Here, the fifteen excited states $|(|2\rangle - |-2\rangle)/\sqrt{2}, S_z = M_S\rangle$, $|\pm 1, S_z = M_S\rangle$ have the same energy corresponding to $E_0 - E_n = -\Delta$. The 10×10 spin-orbit matrix easily obtained from (5) splits into four blocks given in units of $-3\lambda^2/\Delta$ by:

$$\begin{vmatrix} 6 & 0 & \sqrt{2} \\ 0 & 6 & \sqrt{2} \\ \sqrt{2} & \sqrt{2} & 6 \end{vmatrix} \quad \begin{vmatrix} 2 & 0 & \sqrt{2} \\ 0 & 2 & \sqrt{2} \\ \sqrt{2} & \sqrt{2} & 2 \end{vmatrix} \text{ and two times } \begin{vmatrix} 3 & \sqrt{3} \\ \sqrt{3} & 5 \end{vmatrix}.$$

Their eigenvalues are respectively 4, 6, 8; 0, 2, 4 and 2, 6. The corresponding levels shifted by $-12\lambda^2/\Delta$ are a doublet of energy 0, two triplets of energy $\pm 6\lambda^2/\Delta$ and two singlets of energy $\pm 12\lambda^2/\Delta$, in agreement with [9].

The tetragonal crystal field lifts the orbital degeneracy of the ground state by 2ε. For symmetrical splitting, the matrices of perturbation in units of $-3\lambda^2/\Delta$ become:

$$\begin{vmatrix} 6+\varepsilon^* & 0 & \sqrt{2} \\ 0 & 6+\varepsilon^* & \sqrt{2} \\ \sqrt{2} & \sqrt{2} & 6-\varepsilon^* \end{vmatrix} \quad \begin{vmatrix} 2-\varepsilon^* & 0 & \sqrt{2} \\ 0 & 2-\varepsilon^* & \sqrt{2} \\ \sqrt{2} & \sqrt{2} & 2+\varepsilon^* \end{vmatrix}$$

$$\text{and two times } \begin{vmatrix} 3+\varepsilon^* & \sqrt{3} \\ \sqrt{3} & 5-\varepsilon^* \end{vmatrix}$$

in which $\varepsilon^* = \varepsilon/(3\lambda^2/\Delta)$. The eigenvalues are respectively $6+\varepsilon^*, 6 \pm \sqrt{(4+\varepsilon^{*2})}; 2-\varepsilon^*, 2 \pm \sqrt{(4+\varepsilon^{*2})}$ and $4 \pm \sqrt{(4-2\varepsilon^*+\varepsilon^{*2})}$. The corresponding levels shifted by $-12\lambda^2/\Delta$ are two singlets $\pm(3\lambda^2/\Delta)(2 - \sqrt{(4+\varepsilon^{*2})})$, two doublets $\pm(3\lambda^2/\Delta)\sqrt{(4-2\varepsilon^*+\varepsilon^{*2})}$, two singlets $\pm(3\lambda^2/\Delta)(2 + \varepsilon^*)$ and two singlets $\pm(3\lambda^2/\Delta)(2 + \sqrt{(4+\varepsilon^{*2})})$. At $\varepsilon^* \gg 1$, these four latter singlets collapse into two doublets and two groups of three levels are obtained. The upper one consists of two doublets $\varepsilon + 6\lambda^2/\Delta, \varepsilon - 3\lambda^2/\Delta$ and a singlet $\varepsilon - 6\lambda^2/\Delta$ and the lower one is its opposite with two doublets $-\varepsilon - 6\lambda^2/\Delta, -\varepsilon + 3\lambda^2/\Delta$ and a singlet $-\varepsilon + 6\lambda^2/\Delta$ in agreement with equation (2).

References

1. Y. Morimoto, A. Asamitsu, H. Kuwahara, Y. Tokura, Nature **380**, 141 (1996); Y. Morimoto, Aust. J. Phys. **52**, 255 (1999)
2. D.N. Argyriou, T.M. Kelley, J.F. Mitchell, R.A. Robinson, R. Osborn, S. Rosenkranz, R.I. Sheldon, J.D. Jorgensen, J. Appl. Phys. **83**, 6374 (1998)
3. M. Velázquez, A. Revcolevschi, J.-P. Renard, C. Dupas, Eur. Phys. J. B **23**, 307 (2001)
4. C. Zener, Phys. Rev. **82**, 403 (1951)
5. P.W. Anderson, H. Hasegawa, Phys. Rev. **100**, 675 (1955)
6. Q. Huang, A. Santoro, J.W. Lynn, R.W. Erwin, J.A. Borchers, J.L. Peng, R.L. Greene, Phys. Rev. B **55**, 14987 (1997)
7. J. Rodriguez-Carvajal, M. Hennion, F. Moussa, A.H. Moudden, L. Pinsard, A. Revcolevschi, Phys. Rev. B **57**, R3189 (1998)
8. T. Kubo, A. Hirai, H. Abe, J. Phys. Soc. Jpn **26**, 1094 (1969)
9. A. Abragam, B. Bleaney, *Electron Paramagnetic Resonance of Transition Ions* (Clarendon Press, Oxford, 1970), p. 436
10. V. Skumryev, F. Ott, J.M.D. Coey, A. Anane, J.-P. Renard, L. Pinsard-Gaudart, A. Revcolevschi, Eur. Phys. J. B **11**, 401 (1999)
11. G. Matsumoto, J. Phys. Soc. Jpn **29**, 606 (1970)
12. A. Abragam, B. Bleaney, *Electron Paramagnetic Resonance of Transition Ions* (Clarendon Press, Oxford, 1970), p. 431
13. J. Deisenhofer, M.V. Eremin, D.V. Zakharov, V.A. Ivanshin, R.M. Eremina, H.-A. Krug von Nidda, A.A. Mukhin, A.M. Balbashov, A. Loidl, Phys. Rev. B **65**, 104440 (2002)
14. K. Steenbeck, R. Hiergeist, A. Revcolevschi, L. Pinsard-Gaudart, MRS Symposium Proc. **562**, 57 (1999)
15. Y. Suzuki, H.Y. Hwang, S-W. Cheong, R.B. van Dover, Appl. Phys. Lett. **71**, 140 (1997); Y. Suzuki, H.Y. Hwang, S-W. Cheong, T. Siegrist, R.B. van Dover, A. Asamitsu, Y. Tokura, J. Appl. Phys. **83**, 7064 (1998)
16. J. O'Donnell, M.S. Rzchowski, J.N. Eckstein, I. Bozovic, Appl. Phys. Lett. **72**, 1775 (1998)
17. T.K. Nath, R.A. Rao, D. Lavric, C.B. Eom, L. Wu, F. Tsui, Appl. Phys. Lett. **74**, 1615 (1999)
18. F. Tsui, M.C. Smoak, T.K. Nath, C.B. Eom, Appl. Phys. Lett. **76**, 2421 (2000)
19. A.-M. Haghiri-Gosnet, J. Wolfman, B. Mercey, C. Simon, P. Lecoeur, M. Korzenski, M. Hervieu, R. Desfeux, G. Baldinozzi, J. Appl. Phys. **88**, 4257 (2000)

20. K. Steenbeck, T. Habisreuther, C. Dubourdieu, J.-P. Sénateur, Appl. Phys. Lett. **80**, 3361 (2002)
21. M. Kubota, H. Fujioka, K. Hirota, K. Ohoyama, Y. Morimoto, H. Yoshizawa, Y. Endoh, J. Phys. Soc. Jpn **69**, 1606 (2000)
22. J.F. Mitchell, D.N. Argyriou, J.D. Jorgensen, D.G. Hinks, C.D. Potter, S.D. Bader, Phys. Rev. B **55**, 63 (1997)
23. M. Medarde, J.F. Mitchell, J.E. Millburn, S. Short, J.D. Jorgensen, Phys. Rev. Lett. **83**, 1223 (1999)
24. U. Welp, A. Berger, V.K. Vlasko-Vlasov, Qing'An Li, K.E. Gray, J.F. Mitchell, Phys. Rev. B **62**, 8615 (2000)
25. B. Diény, A. Vedyayev, Europhys. Lett. **25**, 723 (1994)
26. A.B. Shick, Phys. Rev. B **60**, 6254 (1999)
27. M. Velázquez, J.M. Bassat, J.-P. Renard, C. Dupas, A. Revcolevschi, J. Phys.: Condens. Matter **14**, 6667 (2002)
28. K. Shimizu, M. Velázquez, J.-P. Renard, A. Revcolevschi, J. Phys. Soc. Jpn **72**, 793 (2003)